Proc. Natl. Acad. Sci. USA
Vol. 90, pp. 4902–4906, June 1993
Biochemistry

Kinetics of $p56^{lck}$ and $p60^{src}$ Src homology 2 domain binding to tyrosine-phosphorylated peptides determined by a competition assay or surface plasmon resonance

GILLIAN PAYNE*, STEVEN E. SHOELSON†, GERALD D. GISH‡, TONY PAWSON‡, AND CHRISTOPHER T. WALSH*

*Department of Biological Chemistry and Molecular Pharmacology, Harvard Medical School, Boston, MA 02115; †Research Division, Joslin Diabetes Center, Department of Medicine, Brigham and Women's Hospital and Harvard Medical School, Boston, MA 02115; and ‡Samuel Lunenfeld Research Institute, Mount Sinai Hospital, Toronto, M5G 1X5 ON, Canada

Contributed by Christopher T. Walsh, February 16, 1993

ABSTRACT **Src homology 2 (SH2) domains are phosphotyrosine-binding modules found within various signal-transducing proteins. We have determined by ^{125}I competition assay and surface plasmon resonance that the SH2 domains of Src and Lck bind to a variety of phosphopeptides with similar affinity and specificity. Both bound with highest affinity [$K_{d(app)} \approx 3.7$ nM; $k_a = 2.4 \times 10^5$ $M^{-1}\cdot s^{-1}$; $k_d = 1.2 \times 10^{-3}$ s^{-1}] a phosphopeptide having a Tyr(*P*)-Glu-Glu-Ile motif found in the hamster polyomavirus middle-sized tumor antigen. Intermediate affinity (5- to 40-fold lower) was observed with phosphopeptides corresponding to the regulatory domains of Src and Lck, containing Tyr^{527} and Tyr^{505}, respectively. Lowest affinity (80- to 300-fold lower) was observed with phosphopeptides corresponding to phosphorylated tyrosines of GTPase-activating protein, insulin receptor substrate 1, and SH2 domain-containing protein-tyrosine-phosphatase 1.**

Src homology 2 (SH2) domains (1, 2) are thought to mediate protein/protein interactions through their ability to bind phosphotyrosine (pY)-containing proteins (3, 4). They are found in a variety of intracellular signaling molecules important for signal transduction (3–6). A sequence alignment of several SH2 domains reveals five highly conserved motifs separated by a less conserved section (3). It is likely that sequence differences dictate specificity of binding to different tyrosine-phosphorylated ligands. Indeed, several examples of SH2 domain specificity have been investigated (7–9) and recent structural information has revealed several potential regions that may confer binding specificity (10–12). A variety of mechanisms have been proposed for SH2-mediated regulation of signal transduction. SH2 domains may recruit substrates to catalytic domains of the proteins in which they reside (13, 14), act as adapter proteins to promote complex formation (15–18), compete with protein-tyrosine-phosphatases to directly regulate the pY content of the cell (19), and regulate catalytic activity (20–24).

Lck is a lymphocyte-specific tyrosine kinase closely related to Src (25). They share SH3, SH2, and catalytic domains, as well as sites of myristoylation and regulatory tyrosine phosphorylation. Phosphorylation of Lck and Src at Tyr^{505} and Tyr^{527}, respectively, suppresses kinase activity (26–28), and tyrosine mutagenesis results in transformation (29, 30). These and other studies suggest a model for regulation in which interaction of the C-terminal pY site with the SH2 domain alters kinase activity (4, 21, 31–33).

We are interested in determining affinity and specificity for phosphoprotein interactions with Lck and Src via their SH2 domains. An important feature of the SH2/phosphoprotein interaction is its ability to be reconstituted with isolated fragments: the intact SH2 domain and a phosphopeptide. Recently this capacity was exploited to affinity-select preferred binding motifs from random phosphopeptide mixtures (34). Both Lck and Src SH2 domains selected the same pYEEI motif, which is distinct from either tail sequence. This motif was found in the hamster polyomavirus middle-sized tumor (hmT) antigen. Individual phosphopeptides corresponding to the hmT sequence, both Lck and Src tail sequences, and various motifs which might direct binding to alternative SH2 domains were prepared. Binding of these phosphopeptides by both Lck and Src SH2 domains was independently assessed by ^{125}I competition assay and surface plasmon resonance (SPR).

MATERIALS AND METHODS

Peptide Synthesis. The synthesis and characterization of phosphopeptides have been described (35, 36). Phosphopeptide nomenclature refers to phosphorylation position in the intact protein (Table 1).

Expression and Purification of Glutathione *S*-Transferase (GST) Fusions to SH2 Domains. The GST fusion vector pGEX-3X (Pharmacia) was modified at the fusion site to insert five glycine residues N-terminal to the factor X site and an *Nde* I cloning site on the C-terminal side of the factor X site to make pGEX-3Xb. PCR was used to generate a DNA fragment coding for the Lck SH2 domain residues 119–224 with a 5′ *Nde* I site and a 3′ *Eco*RI site. The PCR fragment was then ligated into the *Nde* I–*Eco*RI cloning site of pGEX-3Xb to make pGEX-3Xb.lckSH2. The GST–SrcSH2 plasmid was constructed by inserting DNA encoding Src SH2 domain residues 148–251 into the *Bam*HI–*Eco*RI cloning site of pGEX-kT. Overproduction of the GST–LckSH2 and GST–SrcSH2 fusion proteins was accomplished in *Escherichia coli* DH5α. Cells (500 ml) were grown to an OD_{595} of 0.6–0.8 and induced with 2 mM isopropyl β-D-thiogalactopyranoside (Bachem) for 3 hr. Cells were collected by centrifugation and suspended in 10 ml of Hepes-buffered saline (10 mM Hepes, pH 7.5/3.4 mM EDTA/150 mM NaCl) plus 1% (vol/vol) Triton X-100 and 10 mM dithiothreitol. Cells were lysed by two passages through a French press (Aminco–Bowman) at 1200 psi (1 psi = 6.89 kPa) and cellular debris was removed by centrifugation for 20 min at 12,000 × *g*. A 20% ammonium sulfate precipitation was performed on the cell lysate to remove aggregated protein, and the supernatant was purified by glutathione-agarose (Sigma) affinity chromatography (37). The fractions containing GST–SH2 were pooled and concentrated (Centriprep 10, Amicon), and the protein concentration was measured by Bradford assay (Bio-Rad). This procedure routinely produced >95% pure GST–LckSH2 at

The publication costs of this article were defrayed in part by page charge payment. This article must therefore be hereby marked "*advertisement*" in accordance with 18 U.S.C. §1734 solely to indicate this fact.

Abbreviations: SH2, Src homology 2; pY, phosphotyrosine; GAP, GTPase-activating protein; IRS1, insulin receptor substrate 1; SH-PTP1, SH2 domain-containing protein-tyrosine-phosphatase 1; SPR, surface plasmon resonance; GST, glutathione *S*-transferase; hmT antigen, hamster polyoma middle-sized tumor antigen.

Table 1. Relative affinities of phosphopeptides for GST–LckSH2 and GST–SrcSH2

Peptide name*	Sequence	ID_{50}, μM GST–LckSH2	ID_{50}, μM GST–SrcSH2
Lck pY505	TEGQpYQPQP(A)	8.2	58
Src pY527	EPQpYQPGENL	61	66
GAP pY460	DGKEIpYNTIRRK	340	140
hmT pY324	EPQpYEEIPIYL	1.8	1.5
IRS1 pY628	GDGpYMPMSPKS	210	140
SH-PTP1 pY536	ESEpYGNITYPPAMK	470	170

*Names indicate the protein of origin and the position of the pY residue in the protein sequence. GAP, GTPase-activating protein; IRS1, insulin receptor substrate 1; SH-PTP1, SH2 domain-containing protein-tyrosine-phosphatase 1.

yields of 20–30 mg per liter of cells and GST–SrcSH2 at 40–60 mg per liter of cells. Protein was stored at 4°C for immediate use or frozen in liquid nitrogen and stored at −80°C.

Competition Binding Assay. The assay was conducted essentially as described (36). A phosphopeptide derived from hmT antigen (hmT pY324) was radiolabeled with ^{125}I at the N terminus by using Bolton–Hunter reagent (ICN) and was purified by HPLC. GST–SH2 domain (1 μM) and ^{125}I-hmT pY324 (50,000–100,000 cpm) in 20 mM Tris·HCl, pH 7.4/250 mM NaCl/10 mM dithiothreitol/0.1% bovine serum albumin were incubated in the presence of 0–1 mM competing unlabeled phosphopeptide. Assay volumes were 100 μl, to which was added 25 μl of a 20% (vol/vol) solution of glutathione-agarose. The binding of GST to glutathione-agarose and phosphopeptide to SH2 domain was allowed to proceed with vigorous shaking for 12 hr. After incubation, the samples were centrifuged to pellet the agarose and the supernatants were removed by aspiration. The ^{125}I-labeled phosphopeptide remaining bound to the GST–SH2 domain was quantified with a γ counter. Background cpm resulting from ^{125}I-labeled phosphopeptide binding in the absence of SH2 domain were subtracted for each sample.

Binding Interaction Measured by SPR. The Pharmacia Biacore is an instrument that uses SPR to measure interactions (38). Sensorchips CM5 and necessary immobilization reagents were provided by the manufacturer. The Biacore biosensor uses SPR to probe the refractive index change in a flow cell due to the binding of molecules to immobilized ligand (39). Light, impinging on a gold surface between layers with two different refractive indices, resonates with outer shell electrons (plasmons), resulting in a decrease in reflected light intensity under conditions of total internal reflection. This resonance is very sensitive to several parameters, including the refractive index of the medium (the flow cell). If all parameters are held constant, a change in refractive index is detected as a change in reflected light intensity. Since protein mass determines refractive index regardless of sequence, the change in light intensity is directly proportional to the protein mass bound to ligand. The conditions for immobilization of phosphopeptides to the sensorchip surface have been described (42).

Kinetic Analysis of SPR Measurements. The association of a molecule to surface-bound ligand can be described by $dR/dt = k_aCR_{max} - (k_aC + k_d)R_t$ where k_a is the association rate constant, k_d the dissociation rate constant, R_{max} the maximum response when ligand is saturated with bound analyte, R_t the response at time t, and C the concentration of analyte passing over the ligand surface in the flow cell (Pharmacia Biosensor Biacore methods manual). A plot of dR/dt vs. R_t gives a line with slope $-(k_aC + k_d)$, which is equal to $-k_s$. If k_s is plotted against C for various concentrations of analyte the resulting slope is equal to k_a.

The dissociation rate constant k_d is given by the first-order rate equation $dR/dt = k_dR_t$ when the analyte flowing across the flow cell has been replaced with buffer. These measurements are performed when R approaches R_{max}, to minimize the effect of rebinding. Integration of the rate equation gives $\ln(R_{t_1}/R_{t_n}) = k_d(t_n - t_1)$, and a plot of $\ln(R_{t_1}/R_{t_n})$ vs. t for the initial dissociation rate yields a line with slope of $-k_d$.

The equilibrium dissociation constant is $K_d = k_d/k_a$. However, K_d can also be independently determined from equilibrium experiments analogous to Scatchard analysis. When binding equilibrium is reached, $k_a = k_d$ and $dR/dt = k_aC(R_{max} - R_{eq}) - k_dR_{eq} = 0$. Therefore, $k_aC(R_{max} - R_{eq}) = k_dR_{eq}$. Since $K_a = 1/K_d = k_a/k_d$, $R_{eq}/C = K_aR_{max} - K_aR_{eq}$, and a plot of R_{eq}/C vs. R_{eq} yields a line with slope equal to $-1/K_d$.

RESULTS

Relative Affinity of GST–LckSH2 and GST–SrcSH2 for Various Phosphopeptides as Determined by ^{125}I Competition Assay. A high-affinity ligand for both Src and Lck SH2 domains, hmT pY324, was identified by affinity selection from a degenerate phosphopeptide mixture (34) and used as a radiolabeled tracer. Fig. 1 demonstrates the ability of unlabeled phosphopeptides to compete for binding. Data points were experimentally determined and best fit to the data by the equation $y = \{(A - D)/[1 + (x/C)^B]\} + D$ (43),

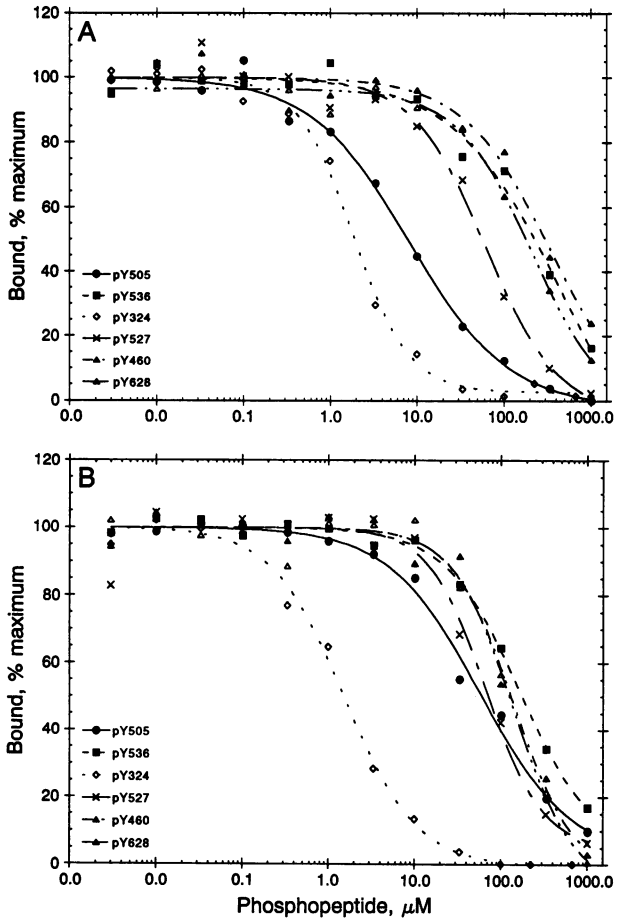

FIG. 1. Competitive binding of phosphopeptides to the Lck (*A*) and Src (*B*) SH2 domains. GST–LckSH2 or GST–SrcSH2 at 1 μM was mixed with ^{125}I-labeled hmT pY324 tracer and various concentrations of competing phosphopeptide (●, Lck pY505; ■, SH-PTP1 pY536; ◇, hmT pY324; ×, Src pY527; ▲, GAP pY460; △, IRS1 pY628) and incubated with glutathione-agarose for 12 hr with shaking. The glutathione-agarose, with bound GST–SH2 domain, was sedimented by centrifugation, the supernatant was removed, and the tracer bound to GST–SH2 domain was quantified by γ counting.

where A = maximum ^{125}I-hmT pY324 remaining bound, B = slope factor, C = ID_{50} (the competing peptide dose resulting in 50% displacement of ^{125}I-hmT pY324), and D = minimum ^{125}I-hmT pY324 remaining bound. The ID_{50} values are listed in Table 1. Because the sensitivity of this assay required that the SH2 domain concentration used be much greater than K_d (estimated from SPR data), the ID_{50} values provide only the *relative* affinity of various phosphopeptides for the SH2 domains.

Both Src and Lck SH2 domains bind the hmT pY324 sequence with equivalent high affinities. All additional phosphopeptides studied bind with lower relative affinity. The phosphopeptides derived from the kinase tails, Lck pY505 and Src pY527, bind with intermediate affinity (5- to 40-fold lower than that of hmT pY324). The remaining phosphopeptides—GAP pY460 (44) SH-PTP1 pY536 (45), and IRS1 pY628 (46), derived from sequences of phosphoproteins thought to interact with other SH2 domains—have even lower relative affinities (80- to 300-fold lower than hmT pY324). Therefore, Src and Lck are able to discriminate among phosphopeptide sequences, and they have remarkably similar binding specificities. The notable exception is that the Lck SH2 domain binds its own tail sequence with higher relative affinity than the Src tail, whereas the Src SH2 domain binds both with equivalently low relative affinities.

Kinetic Analysis by SPR. Although the competition assay described above yielded relative affinities of SH2 domains for phosphopeptides, the ID_{50} values obtained do not represent actual K_d values. For this reason binding experiments were conducted with a Biacore biosensor, which uses SPR to detect binding in real time. The advantage is that with many binding interactions the rate constants k_a and k_d can be determined directly.

The amount of phosphopeptide loaded is crucial for kinetic analysis: too little gives a low signal-to-noise ratio, whereas too much results in ligand titration rather than binding controlled by microscopic rate constants. The presence of an ε-amino group of a peptide lysine was important for adequate loading. Thus a lysine was added to the N terminus of hmT pY324. As a sequence-independent control for the quantity of peptide immobilized, we conducted binding experiments with anti-pY monoclonal antibodies (4G10, kindly provided by Brian Drucker and Tom Roberts, Dana–Farber Cancer Institute). At a flow rate of 5 μl/min, anti-pY at 50 μg/ml was passed over the surface for 10 min (50 μl). The relative responses obtained were 1353 and 3936 response units for hmT pY324 and GAP pY460 surfaces, respectively.

For phosphopeptide/SH2 domain binding experiments, different concentrations of GST–SH2 domain were passed over a sensorchip surface containing covalently bound hmT pY324 or GAP pY460. Binding was monitored by the increase in response units (Fig. 2 *A* and *E*). The early binding phase (<300 sec) can be used to determine k_a. A plot of k_s vs. [GST–SrcSH2] gives a line with slope = k_a (Fig. 2 *B* and *F*; Table 2). At the end of the injection of GST–SrcSH2, buffer passes over the sensorchip surface, rapidly removing dissociated GST–SrcSH2. Thus, this region was analyzed to determine k_d in a plot of $\ln(R_{t_1}/R_{t_n})$ vs. t (Fig. 2 *C* and *F*). K_d was estimated from k_a and k_d and independently from equilibrium data (Table 2). For sensorgrams where equilibria were reached ($dR/dt = 0$), R_{eq}, the response at equilibrium, was estimated by subtracting the response due to bulk refractive index change (≈12 sec after the injection end). K_d values from equilibrium data were obtained by Scatchard analysis (Fig. 2 *D* and *H*; Table 2). No SH2 domain binding was observed either with nonphosphorylated peptides having the same sequences or with GST alone (data not shown). The apparent K_d for binding of GST–SrcSH2 to hmT pY324 (3.5–6.3 nM) is similar to that reported for the binding of the N-terminal SH2 domain of the p85 subunit of phosphatidylinositol 3-kinase (GST–p85N-SH2) to IRS1 pY628 (3.27 nM) (42), suggesting that isolated SH2 domains bind with similar affinities to their cognate phosphopeptides. The apparent K_d estimated for binding of GST–SrcSH2 to GAP pY460 was 22–44 nM (which is lower than predicted from ^{125}I competition data).

Relative Affinity of GST–SrcSH2 for hmT pY324 and GAP pY460 as Measured by SPR. To test whether the Biacore could reliably be used to determine relative binding affinities, a competition assay was developed and the results were compared with those obtained by using the ^{125}I-labeled phosphopeptide tracer. For the Biacore competition assay, hmT pY324 and GAP pY460 were tested for their ability to compete with immobilized hmT pY324 for binding to GST–SrcSH2. GST–SrcSH2 (500 nM) was premixed with various concentrations of free hmT pY324 or GAP pY460 and injected onto the immobilized hmT pY324 sensorchip surface (Fig. 3 *A* and *B*). The amount of GST–SrcSH2 remaining bound to the surface phosphopeptide (R_{eq}) was determined as described above and plotted in Fig. 3*C*.

The results show that GAP pY460 has 89-fold lower affinity than hmT pY324 for GST–SrcSH2, in excellent agreement with the ^{125}I competition assay results showing 93-fold lower affinity (Table 2). Thus, the Biacore gives accurate relative affinities when used in a competition assay. It is not understood why the apparent K_d values determined by direct measurement of k_a and k_d fall in a smaller range than predicted by the competition assays. Possibly, the proximity of the immobilized phosphopeptide to the highly negatively charged carboxymethylated dextran surface causes binding artifacts which are not observed in an SPR competition assay because the observed binding decrease is the result of binding to *free* phosphopeptide.

DISCUSSION

SH2 domains mediate the physical association of pY-containing proteins with downstream effector enzymes. Therefore, understanding the basis of specificity inherent in these interactions may provide valuable insights into discriminating divergent signaling pathways. The interactions of the p85 subunit of phosphatidylinositol 3-kinase with various phosphoproteins have been characterized extensively and provide a model system for analyzing SH2 protein/phosphoprotein interactions generally. A variety of proteins interacting with p85 contain the consensus sequences pYMXM or pYVXM; this tetrapeptide motif confers specificity to p85 SH2 interactions (4, 36, 47, 48). Based on this concept, Cantley and coworkers (34) prepared a phosphopeptide library that was degenerate at pY + 1, pY + 2, and pY + 3 positions and used it to determine specificities of other SH2 domains. For Src, Lck, and additional Src-family SH2 domains, the preferred motif was pYEEI, a sequence found in hmT antigen and other proteins (34). By direct binding analyses we have determined that both Lck and Src SH2 domains bind with similar high affinity to a phosphopeptide corresponding to the hmT sequence. The apparent affinities of Src and Lck for the hmT pY324 peptide are equivalent to that of the p85 N-terminal SH2 for corresponding pY(M/V)XM phosphopeptides (36, 42).

Previous studies have suggested that pY residues in the C-terminal tails of Src and Lck might bind to their own SH2 domains to regulate kinase activity (4, 21, 31–33). Phosphopeptides corresponding to these motifs bind to the SH2 domains with lower relative affinity than the hmT sequence. Nevertheless, with the possibility of multiple phosphoproteins competing for binding to the SH2 domains of Src or Lck, lower relative affinity may be required to offset the advantage of a potential intramolecular interaction and the resulting elevated local concentrations.

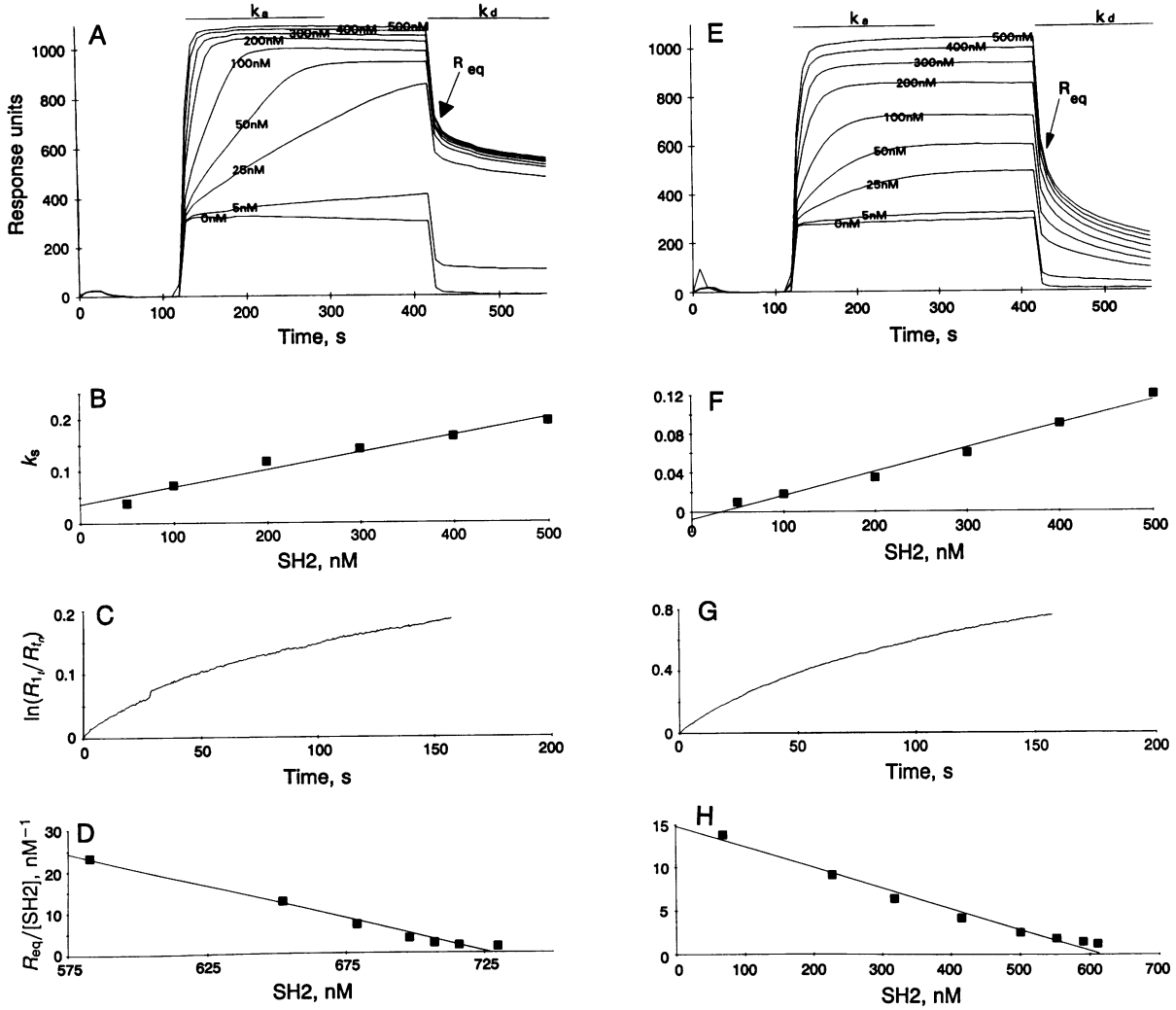

FIG. 2. Kinetic and thermodynamic constants of GST–SrcSH2 binding to hmT pY324 (*A–D*) and GAP pY460 (*E–H*), determined by SPR. Various concentrations of GST–SrcSH2 were passed over an immobilized hmT pY324 or GAP pY460 surface for 5 min at a flow rate of 5 μl/min. The sensorgrams for pY324 (*A*) and pY460 (*E*) are shown with the SH2 concentration indicated. The regions (lines) used to determine k_a and k_d, and the R_{eq} data point (arrow) used to determine K_d, are also shown. k_a (*B* and *F*) and k_d (*C* and *G*) were determined from the slopes of k_s vs. [GST–SrcSH2] and $\ln(R_{t_1}/R_{t_n})$ vs. time, respectively. K_d values for pY324 (*D*) and pY460 (*H*) were determined by Scatchard analysis. The correlation coefficients for the linear regression fits are as follows: *B*, 0.983; *C*, 0.971; *D*, 0.991; *F*, 0.992; *G*, 0.981; *H*, 0.988.

Recent structural analyses of complexes of both Src and Lck SH2 domains with the hmT pY324 peptide (10, 11) provide a framework for understanding phosphoprotein/SH2 interactions. Peptide residues −2 to +4 (relative to pY) contact the SH2 domains, with the side chains of pY and Ile^{+3} occupying deep pockets of either SH2 domain surface. Glu^{+1} and the Glu^{+2} backbone rest on complementary van der Waals surfaces. Both library screening and x-ray crystallographic findings suggest that hydrophobicity at the +3 position is crucial and that isoleucine is favored. To test the importance of the pYEEI motif for tight binding, we determined relative affinities of Src and Lck SH2 domains for additional phosphopeptides which might meet these criteria: GAP pY460, SH-PTP1 pY536, and IRS1 pY628, having pYNTI, pYGNI, and pYMPM motifs, respectively. Surprisingly, each of these peptides bound to both SH2 domains with 80- to 300-fold reduced relative affinity, comparable to differences seen for nonspecific interactions with p85. Therefore, although pY and Ile^{+3} insert into specific pockets, the presence of these determinants is not sufficient for conferring high-affinity binding. Additional residues either within the motif or flanking it may thus act as negative or positive influences. GAP and Lck interact with one another in a phosphorylation-dependent manner and Lck phosphorylates GAP at Tyr^{460} (40). Low relative affinity of Lck SH2 for GAP pY460 suggests that the interaction is not directed by this SH2-mediated interaction.

Table 2. Rate constants and equilibrium constants for GST–SrcSH2 binding to hmT pY324 and GAP pY460

Phosphopeptide	k_a, $M^{-1}\cdot s^{-1}$	k_d, s^{-1}	K_d*, nM	K_d†, nM
hmT pY324	3.3×10^5	1.2×10^{-3}	3.5	6.3
GAP pY460	2.4×10^5	5.4×10^{-3}	22	44

Constants were determined as described in Fig. 3.
*Calculated from k_d/k_a.
†Determined from equilibrium data.

As isolated SH2 domains, Lck and Src bind phosphopeptides with near-identical specificity. A notable exception is the preferential binding of Lck SH2 to its own tail sequence. Nevertheless, these data support the notion that Lck and Src have overlapping functions despite predominant production in different cell types (refs. 25 and 41 and references therein). Our binding data further confirm that specificity in the SH2/phosphoprotein interaction can be reconstituted with peptide fragments, isolated SH2 domains, and corresponding phosphopeptides (36). It is important to note, however, that both binding specificity and the magnitude of the affinities

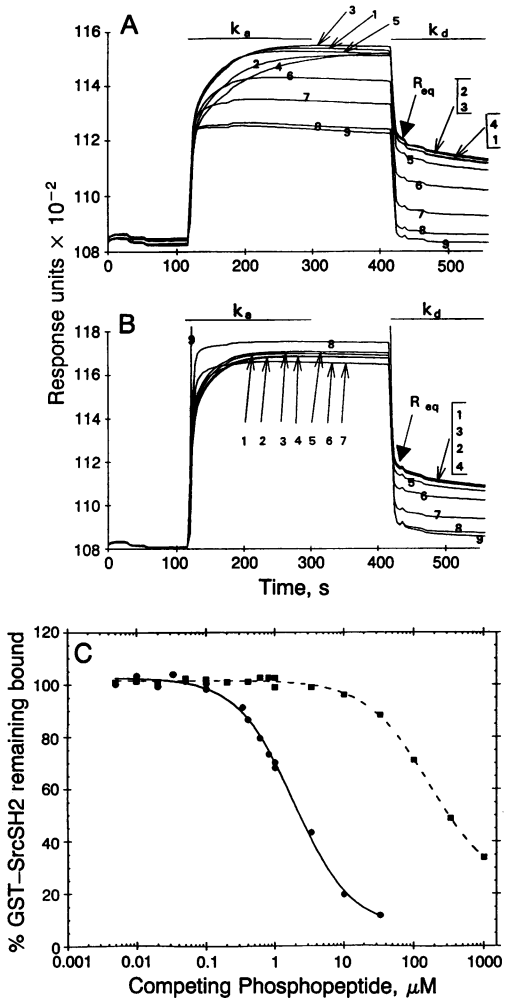

FIG. 3. Competition assay using SPR. GST–SrcSH2 (500 nM) was preincubated with various concentrations of free hmT pY324 (*A*) GAP or pY460 (*B*) and injected over an immobilized pY324 surface. For sensorgrams 1–9 in *A*, concentrations of competing pY324 were as follows: 1, 0 μM; 2, 0.01 μM; 3, 0.033 μM; 4, 0.1 μM; 5, 0.33 μM; 6, 1 μM; 7, 3.3 μM; 8, 10 μM; 9, 33 μM. For sensorgrams 1–9 in *B*, concentrations of competing pY460 were as follows: 1, 0 μM; 2, 1 μM; 3, 3.3 μM; 4, 10 μM; 5, 33 μM; 6, 100 μM; 7, 333 μM; 8, 1000 μM; 9, 3333 μM. The sensorgrams overlap in the 130- to 425-s region because, with increasing competing phosphopeptide concentration, the bulk response increases but the specific binding decreases. The GST–SrcSH2 remaining bound was taken as a percentage of R_{eq} at 0 μM competing phosphopeptide and plotted as standard sigmoidal curves in *C*. ●, pY324; ■, pY460.

may be affected by other domains from the proteins in which the SH2 domains reside.

We are grateful to M. Chaudhuri for the synthesis, purification, and characterization of phosphopeptides and to R. Case for technical assistance. We thank M. Eck, J. Lee, L. C. Cantley, and Z. Songyang for helpful discussion and for communication of unpublished results. This work was supported in part by funds from the National Institutes of Health, the National Science Foundation, and Hoffman–La Roche.

1. Pawson, T. (1988) *Oncogene* **3**, 491–495.
2. Sadowski, I., Stone, J. C. & Pawson, T. (1986) *Mol. Cell. Biol.* **6**, 4396–4408.
3. Koch, C. A., Anderson, D., Moran, M. F., Ellis, C. & Pawson, T. (1991) *Science* **252**, 668–674.
4. Cantley, L. C., Auger, K. R., Carpenter, C., Duckworth, B., Graziani, A., Kapeller, R. & Soltoff, S. (1991) *Cell* **64**, 281–302.
5. Pawson, T. & Gish, G. D. (1992) *Cell* **71**, 359–362.
6. Moran, M. F., Koch, C. A., Anderson, D., Ellis, C., England, L. & Pawson, T. (1990) *Proc. Natl. Acad. Sci. USA* **87**, 8622–8626.
7. Fantl, W. J., Escobedo, J. A., Martin, G. A., Turck, C. W., del Rosario, M., McCormick, F. & Williams, L. T. (1992) *Cell* **69**, 413–423.
8. Kashishian, A., Kazlauskas, A. & Cooper, J. A. (1992) *EMBO J.* **11**, 1373–1382.
9. Reedijk, M., Liu, X., van der Geer, P., Letwin, K., Waterfield, M. D., Hunter, T. & Pawson, T. (1992) *EMBO J.* **11**, 1365–1372.
10. Eck, M., Shoelson, S. E. & Harrison, S. C. (1993) *Nature (London)* **362**, 87–91.
11. Waksman, G., Shoelson, S. E., Pant, N., Cowburn, D. & Kuriyan, J. (1993) *Cell* **72**, 779–790.
12. Williams, K. P. & Shoelson, S. E. (1993) *J. Biol. Chem.* **268**, 5361–5364.
13. Rotin, D., Honegger, A. M., Margolis, B. L., Ullrich, A. & Schlessinger, J. (1992) *J. Biol. Chem.* **267**, 9678–9683.
14. Kim, H. K., Kim, J. W., Zilberstein, A., Margolis, B., Kim, J. G., Schlessinger, J. & Rhee, S. G. (1991) *Cell* **65**, 435–441.
15. Lehmann, J. M., Riethmuller, G. & Johnson, J. P. (1990) *Nucleic Acids Res.* **18**, 1048.
16. Carpenter, C. L., Duckworth, B. C., Auger, K. R., Cohen, B., Schaffhausen, B. S. & Cantley, L. C. (1990) *J. Biol. Chem.* **265**, 19704–19711.
17. Birge, R. B., Fajardo, J. E., Mayer, B. F. & Hanafusa, H. (1992) *J. Biol. Chem.* **267**, 10588–10595.
18. Pelicci, G., Lanfrancone, L., Grignani, F., McGlade, J., Cavallo, F., Forni, G., Nicoletti, I., Grignani, F., Pawson, T. & Pelicci, P. G. (1992) *Cell* **70**, 93–104.
19. Rotin, D., Margolis, B., Mohammadi, M., Daly, R. J., Daum, G., Li, N., Fischer, E. H., Burgess, W. H., Ullrich, A. & Schlessinger, J. (1992) *EMBO J.* **11**, 559–567.
20. Backer, J. M., Myers, M. G., Jr., Shoelson, S. E., Chin, D. J., Sun, X. J., Miralpeix, M., Hu, P., Margolis, B., Skolnik, E. Y., Schlessinger, J. & White, M. F. (1992) *EMBO J.* **11**, 3469–3479.
21. Roussel, R. R., Brodeur, S. R., Shalloway, D. & Laudano, A. P. (1991) *Proc. Natl. Acad. Sci. USA* **88**, 10696–10700.
22. Veillette, A., Caron, L., Fournel, M. & Pawson, T. (1992) *Oncogene* **7**, 971–980.
23. Myers, M. G., Backer, J. M., Sun, X. J., Shoelson, S. E., Miralpeix, M., Hu, P., Margolis, B., Skolnik, E. Y., Schlessinger, J. & White, M. F. (1992) *Proc. Natl. Acad. Sci. USA* **89**, 10350–10354.
24. Shoelson, S. E., Sivaraja, M., Williams, K. P., Hu, P., Schlessinger, J. & Weiss, M. A. (1993) *EMBO J.* **12**, 795–802.
25. Bolen, J. B. & Veillette, A. (1989) *Trends Biochem. Sci.* **14**, 404–407.
26. Piwnica-Worms, H., Saunders, K. B., Roberts, T. M., Smith, A. E. & Cheng, S. H. (1987) *Cell* **49**, 75–82.
27. Veillette, A., Horak, I. D., Horak, E. M., Bookman, M. A. & Bolen, J. B. (1988) *Mol. Cell. Biol.* **8**, 4353–4361.
28. Reynolds, A. B., Vila, J., Lansing, T. J., Potts, W. M., Weber, M. J. & Parsons, J. T. (1987) *EMBO J.* **6**, 2359–2364.
29. Cartwright, C. A., Eckhart, W., Simon, S. & Kaplan, P. L. (1987) *Cell* **49**, 83–91.
30. Marth, J. D., Cooper, J. A., King, C. S., Ziegler, S. F., Tinker, D. A., Overell, R. W., Krebs, E. G. & Perlmutter, R. M. (1988) *Mol. Cell. Biol.* **8**, 540–550.
31. Seidel-Dugan, C., Meyer, B. E., Thomas, S. M. & Brugge, J. S. (1992) *Mol. Cell. Biol.* **12**, 1835–1845.
32. O'Brien, M. C., Fukui, Y. & Hanafusa, H. (1990) *Mol. Cell. Biol.* **10**, 2855–2862.
33. Cooper, J. A., Gould, K. L., Cartwright, C. A. & Hunter, T. (1986) *Science* **231**, 1431–1434.
34. Songyang, Z., Shoelson, S. E., Chaudhuri, M., Gish, G., Pawson, T., King, F., Roberts, T., Sheldon, R., Schaffhausen, B. & Cantley, L. C. (1993) *Cell* **72**, 767–778.
35. Kitus, E. A., Knorr, R., Trzeciak, A. & Bannwarth, W. (1991) *Helv. Chim. Acta* **74**, 1314–1328.
36. Piccione, E., Case, R., Domchek, S. M., Hu, P., Chaudhuri, M., Backer, J. M., Schlessinger, J. & Shoelson, S. E. (1993) *J. Biol. Chem.* **268**, 3197–3202.
37. Smith, D. B. & Johnson, K. S. (1988) *Gene* **67**, 31–40.
38. Malmqvist, M. (1993) *Nature (London)* **361**, 186–187.
39. Granzow, R. & Reed, R. (1992) *BioTechnology* **10**, 390–393.
40. Amrein, K. E., Flint, N., Panholzer, B. & Burn, P. (1992) *Proc. Natl. Acad. Sci. USA* **89**, 3343–3346.
41. Morgan, D. O., Kaplan, J. M., Bishop, J. M. & Varmus, H. E. (1989) *Cell* **57**, 775–786.
42. Felder, S., Zhou, M., Hu, P., Urena, J., Ullrich, A., Chaudhury, M., White, M. F., Shoelson, S. E. & Schlessinger, J. (1993) *Mol. Cell. Biol.* **13**, 1449–1455.
43. De Lean, A., Munson, P. J. & Rodbard, D. (1978) *Am. J. Physiol.* **235**, E97–E102.
44. Trahey, M. & McCormick, F. (1987) *Science* **238**, 542–545.
45. Plutzky, J., Neel, B. G. & Rosenberg, R. D. (1992) *Proc. Natl. Acad. Sci. USA* **89**, 1123–1127.
46. Sun, X. J., Rothenberg, P., Kahn, C. R., Backer, J. M., Araki, E., Wilden, P. A., Cahill, D. A., Goldstein, B. J. & White, M. F. (1992) *Nature (London)* **352**, 73–77.
47. Shoelson, S. E., Chatterjee, S., Chaudhuri, M. & White, M. F. (1992) *Proc. Natl. Acad. Sci. USA* **89**, 2027–2031.
48. Escobedo, J. A., Kaplan, D. R., Kavanaugh, W. M., Turck, C. W. & Williams, L. T. (1991) *Mol. Cell. Biol.* **11**, 1125–1132.